JCI The Journal of Clinical Investigation

Revertant mosaicism in junctional epidermolysis bullosa due to multiple correcting second-site mutations in *LAMB3*

Anna M.G. Pasmooij, Hendri H. Pas, Maria C. Bolling, Marcel F. Jonkman

J Clin Invest. 2007;117(5):1240-1248. https://doi.org/10.1172/JCI30465.

Research Article

Revertant mosaicism due to in vivo reversion of an inherited mutation has been described in the genetic skin disease epidermolysis bullosa (EB) for the genes *KRT14* and *COL17A1*. Here we demonstrate the presence of multiple second-site mutations, all correcting the germline mutation *LAMB3*:c.628G→A;p.E210K, in 2 unrelated non-Herlitz junctional EB patients with revertant mosaicism. Both probands had a severe reduction in laminin-332 expression in their affected skin. Remarkably, the skin on the lower leg of patient 078-01 (c.628G→A/c.1903C→T) became progressively clinically healthy, with normal expression of laminin-332 on previously affected skin. In the other proband, 029-01 (c.628G→A/c.628G→A), the revertant patches were located at his arms, shoulder, and chest. DNA analysis showed different second-site mutations in revertant keratinocytes of distinct biopsy specimens (c.565-3T→C, c.596G→C;p.G199A, c.619A→C;p.K207Q, c.628+42G→A, and c.629-1G→A), implying that there is not a single preferred mechanism for the correction of a specific mutation. Our data offer prospects for EB treatment in particular cases, since revertant mosaicism seems to occur at a higher frequency than expected. This opens the possibility of applying revertant cell therapy in mosaic EB of the *LAMB3* gene by using autologous naturally corrected keratinocytes, thereby bypassing the recombinant gene correction phase.

 Related Commentary, page 1216

Revertant mosaicism in junctional epidermolysis bullosa due to multiple correcting second-site mutations in *LAMB3*

Anna M.G. Pasmooij, Hendri H. Pas, Maria C. Bolling, and Marcel F. Jonkman

Center for Blistering Diseases, Department of Dermatology, University Medical Center Groningen, University of Groningen, Groningen, The Netherlands.

Revertant mosaicism due to in vivo reversion of an inherited mutation has been described in the genetic skin disease epidermolysis bullosa (EB) for the genes *KRT14* and *COL17A1*. Here we demonstrate the presence of multiple second-site mutations, all correcting the germline mutation *LAMB3*:c.628G→A;p.E210K, in 2 unrelated non-Herlitz junctional EB patients with revertant mosaicism. Both probands had a severe reduction in laminin-332 expression in their affected skin. Remarkably, the skin on the lower leg of patient 078-01 (c.628G→A/c.1903C→T) became progressively clinically healthy, with normal expression of laminin-332 on previously affected skin. In the other proband, 029-01 (c.628G→A/c.628G→A), the revertant patches were located at his arms, shoulder, and chest. DNA analysis showed different second-site mutations in revertant keratinocytes of distinct biopsy specimens (c.565-3T→C, c.596G→C;p.G199A, c.619A→C;p.K207Q, c.628+42G→A, and c.629-1G→A), implying that there is not a single preferred mechanism for the correction of a specific mutation. Our data offer prospects for EB treatment in particular cases, since revertant mosaicism seems to occur at a higher frequency than expected. This opens the possibility of applying revertant cell therapy in mosaic EB of the *LAMB3* gene by using autologous naturally corrected keratinocytes, thereby bypassing the recombinant gene correction phase.

Introduction

Reverse mutations in germline or somatic cells bearing an inherited disease-causing mutation can change the phenotype from affected to normal by reexpression of the involved protein. These reverse mutations can be true back mutations — leading to the original wild-type sequence and thus wild-type protein — or can be additional second-site mutations that compensate for the effect of the primary inherited mutation (1). In the latter case, small changes in the amino acid sequence may occur. Revertant mosaicism has been demonstrated for different genetic diseases and in different cell types, as in hepatocytes, lymphocytes, and, in the case of epidermolysis bullosa (EB), keratinocytes (reviewed in refs. 2, 3). EB is a clinically heterogeneous group of heritable blistering disorders leading to fragility of the skin and mucous membranes. The subgroup junctional EB (JEB), characterized by separation at the lamina lucida of the epidermal basement membrane zone (BMZ), is caused by recessive mutations in the genes encoding type XVII collagen (*COL17A1*), integrin α6β4 (*ITGA6* and *ITGB4*), or laminin-332 (LM-332; *LAMA3*, *LAMB3*, and *LAMC2*) (4). Recently, the first instance of correction of EB skin by transplantation of genetically modified epidermal stem cells was reported for a compound heterozygous carrier of laminin β3 (*LAMB3*) mutations (5).

Revertant mosaicism in EB due to in vivo reversion of somatic cells has been described for the genes *COL17A1* and *KRT14* (6–10). The first reported case involved the reversion of one of the defective *COL17A1* alleles into a wild-type sequence due to a mitotic gene conversion event (6). In a second EB patient, the focal expression of type XVII collagen in the skin was the result of a second-site frame-restoring *COL17A1* mutation (7). Recently, we demonstrated the occurrence of multiple correcting *COL17A1* mutations in distinct type XVII collagen–positive skin patches in 2 unrelated probands (10). Amelioration of the EB phenotype can also be achieved on the RNA level by exon skipping, although this rescuing mechanism usually affects the whole body without a mosaic distribution (11–13). In the present study, we describe 2 cases of JEB, caused by germline mutations in the *LAMB3* gene, which appeared to be revertant mosaics. The skin of the left lower leg of patient 078-01 had initially been fragile but reverted so that it no longer had a tendency to blister due to a higher production of LM-332 trimer. Mutation analysis of distinct biopsies revealed in both patients the presence of at least 5 different somatic second-site *LAMB3* mutations that all corrected the same inherited c.628G→A mutation.

Results

Patient 078-01. The proband was a 46-year-old man who consulted our EB center in 1999 with characteristic generalized non-Herlitz JEB features. His clinically normal parents were unrelated, and his siblings were unaffected. There was no family history of inherited skin diseases. Since birth the patient displayed generalized trauma-induced skin blistering that healed with some atrophy and hyperpigmentation. The finger- and toenails were small and short. He had sparse scalp hair with male pattern baldness, mild alopecia of beard hair, and complete loss of eyebrows, eyelashes, and secondary hair. The patient's teeth all had enamel defects (amelogenesis imperfecta) and had been extracted at the age of 20. Remarkably, the proband claimed that after an erosive period of 7 years, the skin of his left lower leg, which had always shown blisters after minor trauma, healed to clinically unaffected skin that was no longer subject to trauma-induced blistering (Figure 1). The reversion of the phenotype occurred after birth and would therefore be classified as

Nonstandard abbreviations used: BMZ, basement membrane zone; EB, epidermolysis bullosa; IF, immunofluorescence; JEB, junctional EB; LAMB3, laminin β3; LDM, laser dissection microscopy; LM-332, laminin-332; R_i, individual information content.

Conflict of interest: The authors have declared that no conflict of interest exists.

Citation for this article: *J. Clin. Invest.* **117**:1240–1248 (2007). doi:10.1172/JCI30465.

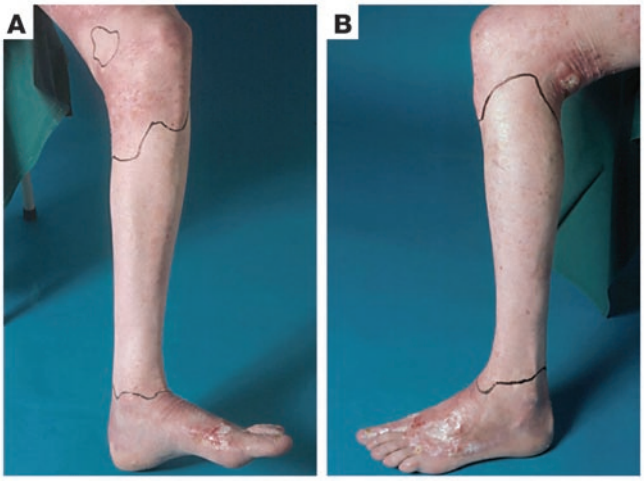

Figure 1
Revertant unaffected skin on the left lower leg of proband 078-01 in January 1999. The skin of the left lower leg reverted to clinically healthy skin after an erosive period of 7 years (**A**, medial aspect; **B**, lateral aspect), while the skin of the right lower leg remained affected. The area of revertant skin is outlined in black.

late-onset revertant mosaicism (3). On the other leg (right) he developed multiple spinocellular carcinomas, for which he was treated by amputation in 1998. One year later, metastasis to lymph nodes and lungs occurred, resulting in death of the patient.

Immunofluorescence (IF) antigen mapping of lesional skin biopsy I (mutant skin [M]) showed subepidermal blister formation with the cleavage plane low in the lamina lucida, characteristic of a LM-332–deficient form of JEB. Type XVII collagen was exclusively present in the blister roof and type VII collagen in the blister base. LM-332 was found, although at a reduced level, in both roof and floor. Nonlesional affected skin biopsy II (M) showed reduced binding of LM-332–specific mAbs GB3 and K140 (Figure 2, A and B) and absent binding of 19-DEJ-1 — the marker for JEB — along the whole dermo-epidermal junction. Surprisingly, sections of biopsy II (M) revealed a small stretch of approximately 25 revertant basal cells that displayed normal LM-332 staining comparable with that of normal age-matched control skin (Figure 2C). Interestingly, both biopsies of unaffected skin showed normal LM-332 staining. Biopsy III (reverted skin [R]) — displayed a mosaic pattern of stretches of normal (3+) and reduced (1+) staining (Figure 2D), while biopsy IV (R) had completely normal 3+ staining (data not shown). Consistent with these findings, 19-DEJ-1 staining was intermittently positive in biopsy III (R) and completely normal in biopsy IV (R).

Electron microscopy of lesional skin demonstrated a subepidermal blister consistent with JEB at the level of the lamina lucida. The blister floor was covered by the lamina densa, and remnants of tonofilaments were present in the blister cavity. Nonlesional affected skin showed a reduced number of hypoplastic hemidesmosomes and less projection of tonofilaments than normal skin (Figure 3A). The lamina densa displayed many duplications and blind "offshoots." In contrast, the hemidesmosomes were normal in shape in revertant skin (Figure 3B), and the lamina densa showed fewer duplications and offshoots.

Mutation detection was performed on *LAMA3*, *LAMB3*, and *LAMC2*, encoding the 3 chains of LM-332. Sequence analysis revealed compound heterozygosity for 2 mutations in the *LAMB3* gene in the proband's genomic DNA: the common nonsense mutation c.1903C→T;p.R635X in exon 14; and c.628G→A;p.E210K in exon 7. Since the latter mutation occurs at position –1 of the 5′ donor splice site of intron 7, an effect on mRNA splicing can be expected (14).

To investigate the reversion mechanisms, mutant (reduced expression) and revertant (normal expression) keratinocytes were separately isolated after K140 immunostaining by laser dissection microscopy (LDM). DNA analysis was carried out on the mutation-bearing exons 7 and 14 and on the neighboring exons 6, 8, 13, and 15 (Figure 4A). In the lower leg biopsy IV (R), both mutations, in exon 7 and 14, were still present. Approximate to the germline mutation, we found a second-site mutation in intron 7, c.628+42G→A, 42 nt downstream of the exon/intron 7 border (Figure 4C). Since biopsy III (R) with a mosaic reversion pattern was also taken from the lower leg, we expected to find the same second-site mutation in the revertant keratinocytes. Surprisingly, c.628+42G→A was not present; instead, another nucleotide change — c.596G→C;p.G199A — in exon 7 was observed (Figure 4B). Cloning and sequencing revealed that this additional transversion (c.596G→C) was located on the same allele as the inherited splice site mutation in exon 7. No other nucleotide changes were identified in either of the 2 revertant biopsy specimens. Furthermore, in fibroblasts taken from the same biopsies and in DNA of more than 80 control subjects, the compensatory second-site mutations were absent. Unfortunately, the amount of 25 revertant cells in biopsy II (M) was too low to allow successful DNA analysis. Only 1 sample could be isolated, while we typically perform our sequence analyses on at least 3 separately isolated samples.

To determine the effect of the germline mutation and the additional substitutions on mRNA splicing, we isolated RNA directly from skin sections. cDNA was then synthesized and analyzed by nested RT-PCR using exonic primers that amplified nt 580–848 of *LAMB3* cDNA. In addition to the full-length mRNA transcript (269-bp amplimer), the RNA isolated from affected skin revealed the presence

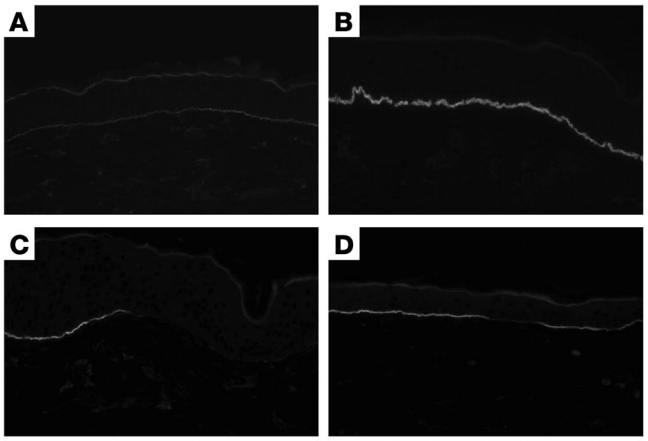

Figure 2
IF microscopy reveals cellular mosaicism in the skin of proband 078-01. (**A** and **B**) Staining with monoclonal antibody K140 to the β3 chain of LM-332 was markedly reduced in affected skin of the upper arm (**A**) compared with normal control skin (**B**). (**C**) To our surprise, a short stretch of approximately 25 basal cells embedded in an LM-332–reduced environment that stained brightly for LM-332 was observed in biopsy II (M). (**D**) Biopsy III (R) of the left lower leg showed an interrupted pattern, with normal and reduced staining along the epidermal-dermal junction, while biopsy IV (R) revealed bright staining for all basal cells (data not shown). Original magnification, ×40.

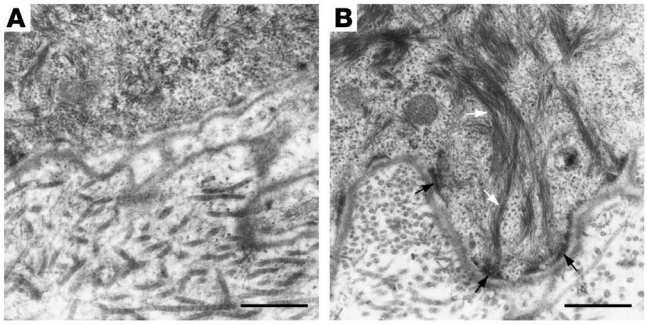

Figure 3
Normal hemidesmosomes in revertant skin. (**A**) Ultrastructural examination of the affected skin of proband 078-01 showed a reduced number of abnormal hemidesmosomes. The intermediate filaments were not connected to the flattened basilar cell periphery. (**B**) The revertant skin of the lower leg reveals intermediate filaments that connect to normal hemidesmosomes in the basilar cell periphery. Black arrows indicate hemidesmosomes and white arrows intermediate filaments. Scale bars: 500 nm.

of 3 aberrant mRNA transcripts: (i) an out-of-frame transcript lacking exon 7; (ii) a transcript with the deletion of exon 7 together with the first 2 nt (AG) of exon 8; and (iii) an in-frame mRNA transcript lacking exon 7 and the first 101 nt of exon 8 (Figure 5, A and B). These 3 alternative mRNA transcripts with deletions of, respectively, 64, 66, and 165 bp, were previously described for the 628G→A mutation by Pulkkinen et al. (14). Detection of their fourth transcript lacking 210 bp was not feasible with our primer set.

Interestingly, a slower migrating amplimer was visible in the RNA isolated from biopsy IV (R). Subsequent cloning and sequencing showed retention of the first 66 bp of intron 7 in this 335-bp product (Figure 5B). In previous work, RNA isolation of mosaic skin biopsy specimens was carried out by staining every fourth tissue section and subsequently using this staining pattern for selection of desired cells from the intermittent sections by LDM isolation (10). Such an approach requires stretches of mutant and revertant cells of sufficient length. Since in biopsy III (R), the areas of reduced and bright staining alternated over short distances — sometimes fewer than 10 basal cells — (Figure 2D), we instead chose to use the whole biopsy for RNA analysis, bearing in mind that about 50% of the cells had normal and 50% reduced LM-332 staining. As expected, RNA of biopsy III (R) had a distribution of mRNA transcripts (Figure 5A, lane 4) different from that of RNA from the affected skin biopsies. The

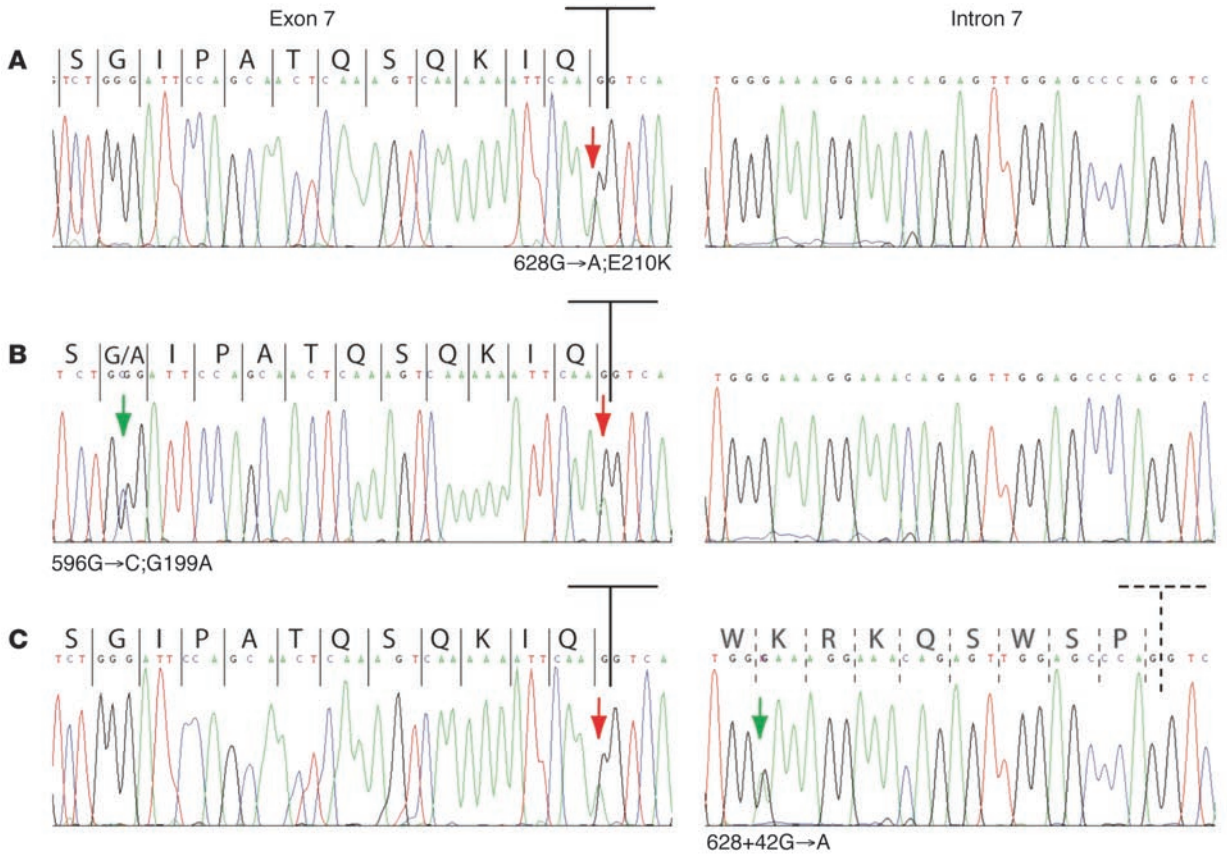

Figure 4
Identification of the different correcting *LAMB3* mutations in patient 078-01. (**A**) The G→A nucleotide change at position –1 of the 5′ splice site of intron 7 was present in keratinocytes with reduced staining of LM-332. (**B**) The second-site mutation c.596G→C was present in revertant keratinocytes of biopsy III (R). (**C**) An additional mutation in intron 7, c.628+42G→A, in revertant keratinocytes of biopsy IV (R). The cryptic splice site, CAG|GT, which is used when the c.628+42G→A substitution is present, is indicated by the dashed line. Red arrows indicate the inherited mutation, and green arrows the second-site mutations. Corresponding amino acid sequences are indicated above the nucleotide sequences.

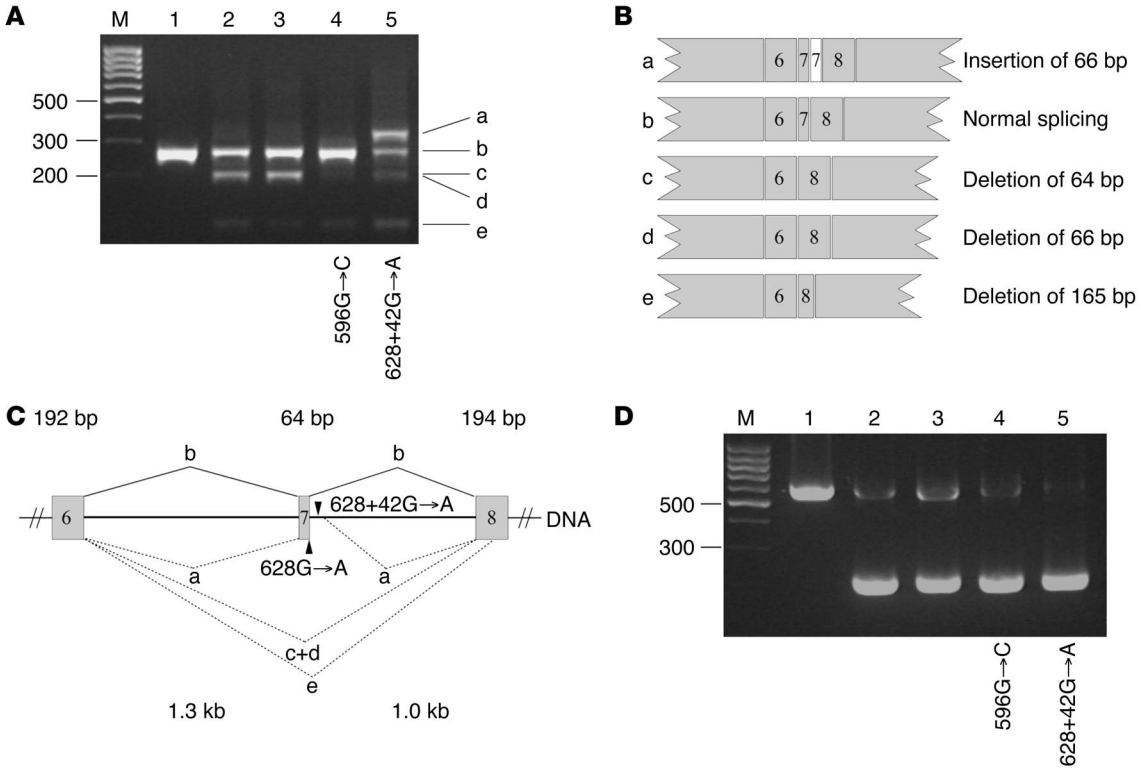

Figure 5
Effects of second-site mutations at the mRNA level (patient 078-01). (**A**) nt 580–848 of *LAMB3* mRNA was analyzed by RT-PCR. Along with the expected 269-bp product in the control sample (lane 1), affected skin samples revealed 3 smaller transcripts (lanes 2 and 3). Isolation and sequencing showed the presence of normally spliced transcript (**B**, b), the exon 7–deleted transcript (c), a transcript missing the first 2 nt of exon 8 in addition to exon 7 (d), and a transcript with a deletion of 165 nt, comprising exon 7 and the first 101 nt of exon 8 (e), in biopsy I (M) (lane 2) and biopsy II (M) (lane 3). In the mosaic biopsy III (R) (lane 4), the normally spliced variant was more abundant, whereas the amount of aberrant mRNA transcripts was decreased. In the completely reverted biopsy IV (R), an additional transcript retaining the first 66 nt of intron 7 (**B**, a) was present (lane 5). (**C**) The *LAMB3* gene, with sizes of exons (above) and introns (below). Splicing of normal full-length transcript is indicated with the solid line (**C**, b). Dotted lines depict the splicing of aberrant transcripts (**C**, a, c, d, and e). The mutations c.628G→A and c.628G+42G→A are indicated by black arrowheads. (**D**) p.R635X induces exon 14 skipping. Primers amplifying bp 1,641–2,229 demonstrated the 589-nt transcript in the control (lane 1). This fragment was almost absent in all patient biopsies (lanes 2–5), while a smaller amplimer of 210 bp was visualized. Lane M contains a 100-bp molecular size marker (**A** and **D**).

amplimers that resulted from alternative splicing due to the transition in the last nucleotide of exon 7 were less abundant (Figure 5B, transcripts c–e), while the 269-bp amplimer from normal splicing dominated. Cloning of these normal-sized amplimers showed that almost all clones carried both c.596G→C and c.628G→A.

Nested RT-PCR was also performed with oligonucleotides amplifying bp 1,641–2,229 of *LAMB3* cDNA surrounding the other inherited mutation, c.1903C→T;p.R635X. Normal human controls demonstrated a clear 589-bp PCR product, while in all patient biopsies, expression of this product was reduced (Figure 5D). An additional faster-migrating 210-bp amplimer originated from an out-of-frame transcript with a deletion of exon 14 (379 bp) and is therefore prone to nonsense-mediated RNA decay. There were no differences in mRNA or DNA between the unaffected and affected skin biopsies. Thus, reversion of the inherited p.R635X mutation did not occur.

Patient 029-01. The germline mutation of the second non-Herlitz JEB proband, 64 years old at the time of publication, has been described elsewhere (14, 15). His consanguineous parents were unaffected, but his sister has the same disease. The grandparents were first cousins. IF of nonlesional affected skin specimens showed severely reduced LM-332 expression, while type XVII collagen staining was normal (15). Consistent with this finding, electron microscopic analysis of nonlesional affected skin showed hypoplastic hemidesmosomes (15). Mutation screening identified the homozygous c.628G→A transition (14).

Because we have observed multiple reversion events in EB patients (10), we ask patients in our EB clinic on a routine basis whether they have patches of clinically unaffected skin. In early 2006, patient 029-01 indicated several unaffected regions at his arms, shoulder, and chest (Figure 6). Unfortunately, he could not remember how long these patches had been present and whether they had increased in size over time. Older photographic material was lacking. IF microscopy of all 4 biopsies of unaffected skin showed keratinocytes with bright staining comparable to that of normal control skin (data not shown), thereby confirming that this EB patient was another individual with revertant mosaicism. Consistent with this finding, in the revertant skin, the number of hemidesmosomes was normal, in contrast to the reduced amount in the mutant skin.

Subsequent DNA analysis of the revertant keratinocytes by nested PCRs of exons 5–9 revealed different second-site mutations in

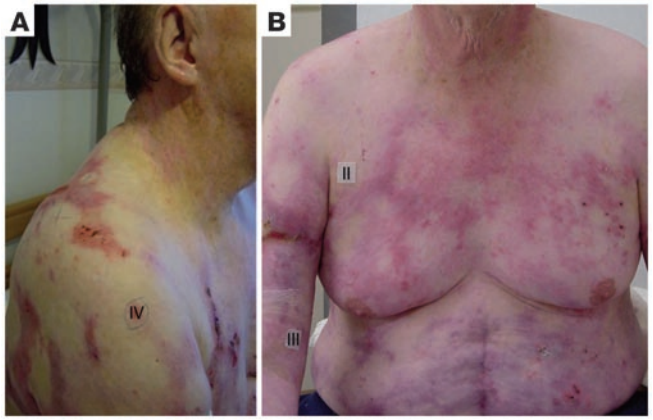

Figure 6
Revertant unaffected skin on upper arm and shoulder of non-Herlitz JEB patient 029-01 in January 2006. (**A**) The region where biopsy IV (R) was taken is circled, whereas other skin areas without blistering tendency are indicated with crosses. The latter are clearly distinguishable from the surrounding erythematous atrophic skin. (**B**) Frontal aspect of the chest. The sites of biopsy II (R) and III (R) are labeled.

different biopsy specimens — c.565-3T→C, c.619A→C;p.K207Q, and c.629-1G→A — that were not present in the keratinocytes with reduced staining, nor in more than 160 chromosomes of control subjects (Figure 7). Despite extensive sequencing of exons 5–9, the reversion mechanism in biopsy II (R) could not be detected. Most probably another second-site mutation was present, as the revertant cells remained homozygous for the c.628G→A mutation (data not shown).

The effect of the second-site mutations on the mRNA was investigated by RT-PCR using primers that amplified nt 580–848 (Figure 8). In biopsy I (R), the relative level of the 269-bp amplimer, which here contained both the c.619A→C and the c.628G→A mutations, was increased compared with the level of the 269-bp amplimer in affected skin that only contained the c.628G→A mutation (Figure 8, lane 1). In the 2 other biopsies — II (R) and III (R) — the distribution of mRNAs was also altered in favor of the full-length mRNA transcript. In biopsy IV (R), having the additional c.629-1G→A mutation located in the acceptor splice site of intron 7, more of the in-frame 66 bp–deleted transcript was produced (Figure 5B, band d). This shorter in-frame transcript results in a smaller, but probably functional, LM-332 protein that is able to restore skin function.

Discussion

This study in 2 patients with non-Herlitz JEB describes for the first time to our knowledge revertant mosaicism of LM-332 (Figure 9A). The identification of different second-site mutations again demonstrates that single individuals can undergo multiple reversion events (10, 16, 17). All rescue mechanisms involved nucleotide changes in the DNA: c.565-3T→C, c.596G→C;p.G199A, c.619A→C;p.K207Q, c.628+42G→A, and c.629-1G→A (Figure 9B). The second-site mutations had effects at the RNA level and thereby at the protein level.

The inherited G→A transition at the last base of exon 7 (c.628G→A) converts a negatively charged glutamic acid residue into a positively charged lysine (p.E210K). This substitution takes place within the N-terminal globular domain of the short arm of the LM-332 β3 chain, which has been postulated to be critical in the association of LM-332 with other structural proteins of the BMZ, including laminin-311 (18). Such polarity change may disturb protein-protein interactions of LM-332 and reduce epidermal-dermal adhesion. A more profound effect is observed on mRNA splicing, as the 628-nucleotide change takes place in the consensus sequence at the 5′ splice site (14, 19, 20). The c.628G→A mutation generates 4 additional aberrant transcripts as described by Pulkkinen et al. (14). RNA splicing is directed by the 5′ donor splice site, the 3′ acceptor splice site, and the branch point sequence that is located 18–40 nt upstream of the acceptor splice site (reviewed in ref. 21). In the human genome, these splicing sequences are poorly conserved; only the GT at the 5′ end of the intron, AG at the 3′ end of the intron, and branch point adenosine at the 2′ position are almost invariable. Since natural splice sites can be different from the consensus sequence, both splice site strength and accessory regulatory sequences influence splice site selection. Various web-based resources for splice site prediction are available, such as Automated Splice Site Analyses, located at https://splice.cmh.edu. Computational analyses of our *LAMB3* genomic sequences showed that the c.628G→A mutation weakens the individual information content (R_i) of the natural donor site from 8.2 to 5.1 bits. Besides this 5′ splice site, 2 other donor sites with a high R_i value were present in the analyzed sequence. These sites were TGG | GT, with an R_i of 4.3 bits, and CAG | GT, with an R_i of 3.2 bits, located 37 and 66 nt downstream of the natural exon/intron 7 border, respectively.

The second-site mutation c.628+42G→A lowered the R_i value of the alternative donor site TGG | GT drastically from 4.3 to 0.8 bits, whereas the CAG | GT site remained unchanged at 3.2 bits. The weakening of the TGG | GT donor site might favor use of the cryptic CAG | GT site by the spliceosome, thereby resulting in the observed larger mRNA transcript with retention of the first 66 nt of intron 7. The in-frame insertion led to incorporation of a stretch of 22 amino acids — SQCGYFSCPWNYGWKRKQSWSP — in the N-terminal domain of the β3 chain. Although this stretch contained 2 amino acids with basic side chains, 4 with acidic side chains, and 6 with bulky aromatic side chains, the resulting LM-332 protein was apparently functional, as it resulted in reversion of the skin phenotype.

The second-site c.596G→C changed a glycine to alanine at amino acid position 199, and second-site c.619A→C changed a lysine to glutamine at position 207. More importantly, both also affected mRNA splicing, as more normal-sized transcripts were present in the revertant cells. Computational analyses did not demonstrate effects on R_i values of the splice sites used. We also excluded the possibility that the mutations altered exonic splicing enhancer (ESE) sequences using RESCUE-ESE software (http://genes.mit.edu/burgelab/rescue-ese). ESEs enhance splicing when present downstream of a 3′ splice site and/or upstream of the 5′ splice site (22). A third factor that may influence splice site selection is a possible effect of these second-site mutations on the RNA secondary structure that contains the c.628G→A mutation. Single nucleotide alterations can affect the secondary structure of RNA, which in turn can influence RNA splicing (23, 24).

Two nucleotides downstream of the wild-type 3′ acceptor site of intron 7, CAG | AG, a cryptic splice site, GAG | GT, was present. Therefore c.628G→A generated not only a 64 bp–deleted transcript, but also the 66 bp–deleted transcript. The second-site mutation 629-1G→A reduced the strength of the natural acceptor site from 10.5 to 2.9 bits, whereas the cryptic splice site increased in strength from 6.0 to 7.8 bits. RT-PCR analysis indeed demonstrated preferential use of the cryptic splice site generating an in-frame rather than an out-of-frame transcript. Translation resulted in a smaller functional β3 polypeptide lacking 22 amino

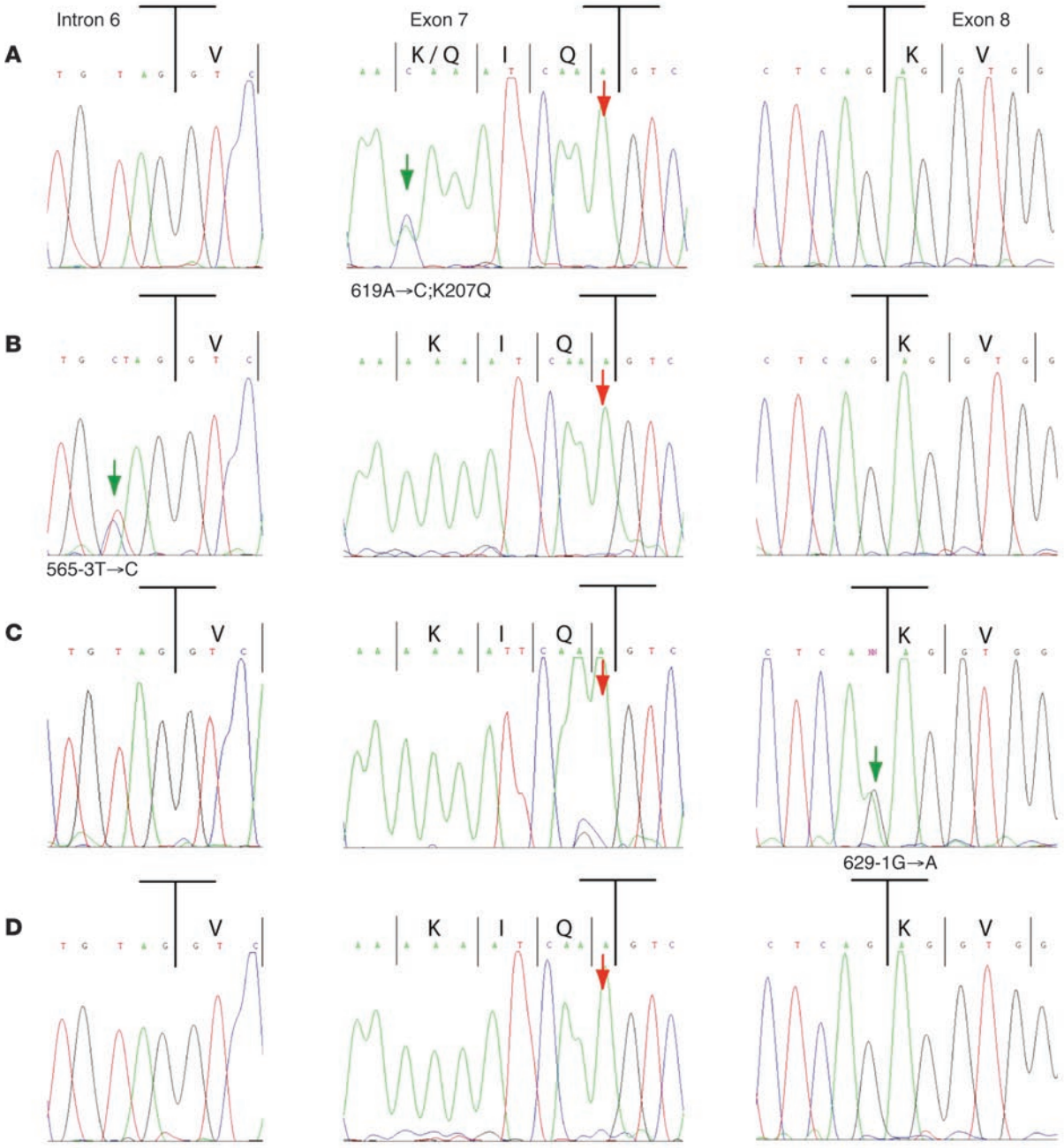

Figure 7
The inherited homozygous c.628G→A mutation was present in 029-01 proband's keratinocytes with normal (**A**–**C**) as well as reduced (**D**) LM-332 staining. (**A**) In biopsy I (R), a second-site mutation, c.619A→C;p.K207Q, was present in exon 7. Biopsy III (R) had an additional substitution, c.565-3T→C, in the 3′ splice site of intron 6 (**B**) and biopsy IV (R) an additional c.629-1G→A change in the 3′ splice site of intron 7 (**C**). (**D**) None of these additional substitutions were seen in LDM-isolated mutant keratinocytes. Red arrows indicate the inherited mutation, and green arrows the second-site mutations. Amino acid sequences are indicated above the nt sequences.

acids within the N-terminal domain of the short arm. The final second-site mutation, c.565-3T→C, was located in the 3′ acceptor site of intron 6 and gave a small increase, from 5.3 to 5.6 bits, in the R_i value. Although small, it might explain the higher production of wild-type mRNA transcript.

The other inherited mutation, p.R635X, which is the most common mutation in JEB patients of European origin, predicts a premature termination codon (PTC) within the coiled-coil rod of the LM-332 protein. The corresponding transcript level is expected to be markedly reduced due to nonsense-mediated RNA decay. RT-PCR around exon 14 indeed showed reduced expression of the 589 amplimers as described by Pulkkinen et al. (25). Also, a smaller migrating 210-bp amplimer was detected for patient 078-01 belonging to an out-of-frame transcript lacking exon 14 (379 nt). Although this nonbeneficial transcript has not been reported before, it is not uncommon that PTCs induce exon skipping (26).

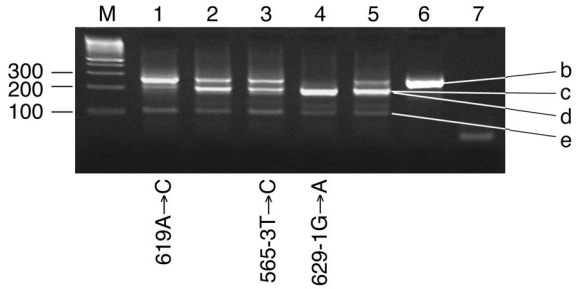

Figure 8
Effects of second-site mutations at the mRNA level (patient 029-01). Oligonucleotide primers were similar to those described in Figure 5. A normal human control sample shows the expected 269-bp product (lane 6). The affected skin sample contained 3 additional smaller fragments due to the c.628G→A transition (lanes 1–4 and Figure 5B, c–e). The revertant keratinocytes of biopsy I (R) with the secondary c.619A→C mutation (lane 1) produced more full-length mRNA transcript and fewer 64 and 66 bp–deleted transcripts than mutant keratinocytes (lane 5). This is also seen in the revertant keratinocytes from biopsy II (R) (lane 2) and biopsy III (R) (lane 3) containing the additional c.565-3T→C mutation. In contrast, the revertant keratinocytes of biopsy IV (R) with the second-site c.629-1G→A mutation had a greater abundance of the transcript with the 66-bp deletion (lane 4). Lane M contains a 100-bp molecular size marker and lane 7 a negative control.

Just over a year ago, several research groups separately identified the phenomenon of multiple in vivo reversions in single individuals, thereby challenging the concept that revertant mosaicism occurs through a single event. Multiple somatic reversions have now been observed for the *FAH* gene in tyrosinemia type I (16); the *RAG1* gene in Omenn syndrome (17); the *CD3*ζ gene in severe combined immunodeficiency disease (27); the *COL17A1* gene in EB (10); and here for the *LAMB3* gene in EB. The number of recognized compensatory second-site mutations in inherited disorders is rapidly growing. Wada et al. (17) described a patient with 6 different second-site mutations, all correcting the same delC mutation in the *RAG1* gene, whereas Rieux-Laucat et al. (27) identified 3 somatic second-site mutations that all reverted the nonsense codon p.Q70X in the *CD3*ζ gene to a missense codon. The mechanism underlying the different second-site mutations in their patients remained unclear. An increased rate of reversion events can be evoked by mutational hot spots such as direct repeats or homonucleotide tracts (28). Therefore, we analyzed the sequences around our second-site mutations. The known CAGG/CCTG mutation hot spot sequence that Levran et al. (29) identified near some point mutations was not in close proximity — defined as more than 10 nt away — to any of the second-site mutations. Homonucleotide tracts were identified for 596G→C, 619A→C, and 628+42G→A, while a short direct repeat was identified for 629-1G→A, showing that the majority of the mutations was caused by misalignment-mediated errors.

Neither of the patients had exposure to chemotherapy or radiotherapy, excluding the possibility that they played a role in the development of these mutations. UV light could be also ruled out as a factor, as neither patient exposed his skin to sunlight, and the signature UV transition mutations, C→T and G→A, were only present in 2 of 5 second-site mutations (30). The cause of the correcting DNA events in our patients thus remains uncertain. It must be random mutagenesis or a yet-unidentified remedial mechanism, and the repair data described here favor the latter.

Arguments in favor of random mutagenesis. The average mutation rate in humans is estimated to be 175 mutations per diploid genome per generation by Nachman and Crowell (31). It may well be that our patients have a higher mutation rate and that therefore different advantageous second-site mutations accumulated in keratinocytes. Other mutations in different genes or in different cell types that are not advantageous for the cell may just get lost. Accordingly, no second-site mutations were detected in peripheral blood or the fibroblast samples. Such an increased mutation rate can be the result of inactivation of a caretaker gene (32). Inactivation results in genetic instabilities, causing an increased mutation rate affecting all genes. In light of this hypothesis, it is interesting to note that both patients developed cancer, which is known to result from an accumulation of somatic mutations (33).

Arguments in favor of a directed mutagenesis. In the heterozygous patient 078-01, all 3 second-site mutations correct the same 628G→A mutation. No second-site mutation was observed for the primary 1903C→T mutation on the other allele. The *FAH* gene patient described by Bliksrud et al. (16) was also heterozygous, and similar to our findings, both in vivo reversions were located on the same allele. No knowledge of the proper wild-type sequence is required to execute the reversion repair mechanism. While it can be argued that in a heterozygous patient, information on the correct sequence is available on the other allele, this can not be the case in a homozygous patient. In 029-01, homozygous for 628G→A, 4 different second-site mutations were identified. Also, the probands described by Wada et al. (17) with 6 different reversions and by Rieux-Laucat et al. (27) with 3 different reversions were both homozygous. More cases of in vivo reversion in homozygous and hemizygous patients have been described previously (2).

Recently, we reported revertant mosaicism for type XVII collagen non-Herlitz JEB (10). In these *COL17A1* mosaic patients, the revertant patches remained stable during life and did not expand. Apparently, the revertant stem cells did not have a selection advantage compared with their deficient counterparts. Therefore, we concluded that the correcting mutations leading to the healthy skin patches of tens of square centimeters in size occurred during embryogenesis. In the *LAMB3* mosaic patients described here, the situation was different. According to patient 078-01, his revertant skin patch increased in size, while patient 029-01 had not noted extension of the healthy skin area. This difference might be explained by the fact that patient 029-01 (c.628G→A/c.628G→A) likely has a higher level of LM-332 production in his deficient cells than patient 078-01 (c.628G→A/p.R635X), because the allele containing the nonsense mutation in the latter was not contributing to the LM-332 production. Therefore, expansion of reverted keratinocytes could indeed have been easier in proband 078-01 than in 029-01, as the deficient cells were less able to compete.

LM-332 is involved in cell locomotion and migration in wound healing (34, 35). Interactions with α2β1 and α3β1 are important for cell attachment, spreading, and migration, whereas binding to α6β4 results in stable anchorage without cell spreading (36, 37). Also, suppression of endogenous LM-332 in an oral squamous cell carcinoma cell line led to decreased cell attachment and increased migration (38). The benefit of reversion is possibly related to the role of LM-332 in migration; however, this potential selection advantage of LM-332 revertant stem cells requires thorough investigation.

The treatment for genetic diseases seems to lie in gene therapy. Mavilio et al. (5) recently showed in a phase I clinical trial the correction of LM-332–deficient JEB by transduction of retroviral

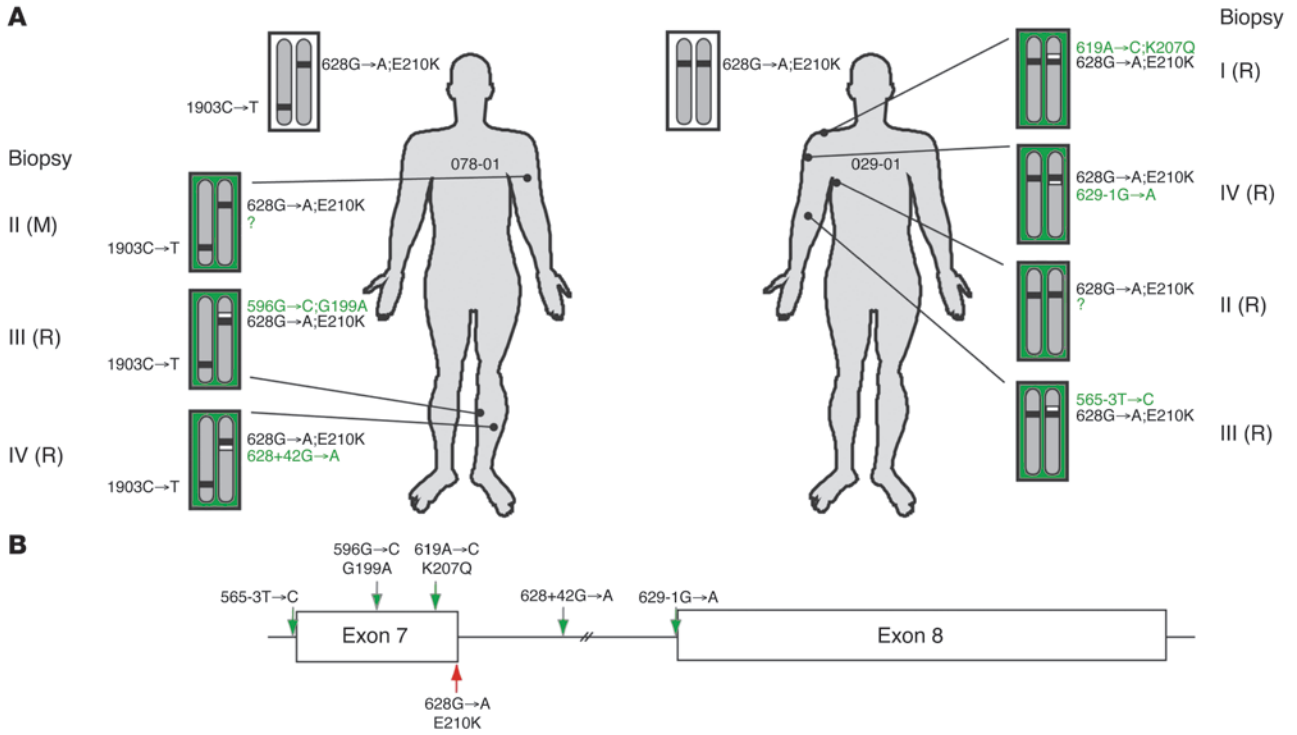

Figure 9
Schematic drawing showing the different second-site mutations that all corrected *LAMB3*:c.628G→A. (**A**) The inherited germline mutation c.628G→A is depicted as black rectangles, while the second-site mutations are depicted as white rectangles. Cells with a mutant phenotype are white, and those with a revertant phenotype green. (**B**) Distribution of the mutations in the *LAMB3* gene. The red arrow indicates the inherited mutation, and green arrows indicate the second-site mutations.

vector expressing β3 cDNA. A 36-year-old man received a transplant of cultured epidermal sheets on both legs after removal of the outer skin layer. Transplantation was successful, as during the first year of follow-up, blistering, infections, inflammations, and an immune response were absent. Revertant mosaicism opens the fascinating possibility of "revertant cell therapy" for mosaic patients using patient's own naturally corrected cells for transplantation. In *LAMB3* revertant mosaic patients, one might take advantage of the patient's own naturally corrected cells for skin transplantation. This autologous cell therapy bypasses the phase of molecular gene correction. Revertant mosaicism was thought to be a rare event, but our recent observations indicate that it might occur at a higher frequency than expected.

Methods

Biopsy sites. From patient 078-01 four 4-mm punch biopsies were taken and snap frozen for IF microscopy: 1 from lesional affected skin from the left upper arm (biopsy I [M]), 1 from nonlesional affected skin from the left upper arm (biopsy II [M]), and 2 from unaffected skin of the left lower leg (biopsies III [R] and IV [R]). For electron microscopy, three 2-mm punch biopsies were taken: 1 from lesional affected skin of the left upper arm, 1 from nonlesional affected skin of the left upper arm, and 1 from unaffected skin of the left lower leg.

The second proband, 029-01, has been described elsewhere, specifically, as patient no. 9 in the publication of Jonkman et al. (15) and as patient no. 2 in the publication of Pulkkinen et al. (14). Six 4-mm punch biopsies were taken for IF microscopy: 1 from unaffected skin from the right shoulder (biopsy I [R]), 1 from unaffected skin of the right side of the chest (biopsy II [R]), 1 from unaffected skin of the right lower arm (biopsy III [R]), 1 from unaffected skin from the right upper arm (biopsy IV [R]), and 2 from nonlesional affected skin from the left upper arm (biopsies V [M] and VI [M]). For electron microscopy, two 2-mm punch biopsies were taken: 1 from nonlesional affected skin of the left upper arm and 1 from unaffected skin of the right upper arm. Informed consent for the scientific use of the material and photographs was obtained from both patients according to the guidelines of the ethics committee of the University Medical Center Groningen and the Declaration of Helsinki.

Immunomorphological analysis of skin and cultured keratinocytes. Details of IF microscopy, electron microscopy, and keratinocyte culturing have been extensively documented elsewhere (39). For detection of LM-332, two antibodies were used: K140 specific to the β3 chain (gift from B. Burgeson, Harvard University, Boston, Massachusetts, USA) and GB3, recognizing a conformational epitope of the γ2 chain (Abcam). As a marker for JEB, we used mAb 19-DEJ-1 (gift from J.D. Fine, Vanderbilt University School of Medicine, Nashville, Tennessee, USA). Type XVII collagen was stained with 1A8C and 1D1 (gifts from K. Owaribe, Nagoya University, Nagoya, Japan), type VII collagen with LH7:2 (gift from I. Leigh, St. Bartholomew's and the Royal London School of Medicine and Dentistry, London, United Kingdom). The Alexa Fluor 488–conjugated goat anti-mouse IgG antibody (Molecular Probes) was used as secondary step with labeled conjugate.

DNA and RNA isolation from skin sections. DNA recovery with LDM was performed as described previously (10). Monoclonal antibody K140 was used to differentiate between keratinocytes with normal and reduced staining. For DNA isolation, about 200 cells were collected in a 0.2-ml reaction tube. Proteinase K digestion was for 60 minutes at 55°C, followed by proteinase K inactivation at 98°C for 15 minutes. The final aliquots were used for

PCR. For RNA isolation, three 10-μm skin sections were lysed in 100 μl of lysis buffer plus 0.7 μl β-mercaptoethanol. Total RNA (15 μl) was then prepared using the Stratagene RNA Microprep kit. cDNA was synthesized as described elsewhere (10).

Identification of the mutations in LDM samples. For *LAMB3* mutation detection in LDM-isolated DNA, we used nested PCR. One microliter of the first PCR was used for the second PCR. PCR cycling conditions were 5 minutes at 94°C, followed by 35 cycles at 94°C for 45 seconds, 55°C for 45 seconds, and 72°C for 1 minute, and a final extension at 72°C for 7 minutes. Water was used as a negative control. Primer sequences used to amplify the different exons of *LAMB3* and expected product sizes are listed in Supplemental Table 1 (supplemental material available online with this article; doi:10.1172/JCI30465DS1). After PCR, aliquots of 14 μl were examined on 1.5% agarose gels. The Department of Medical Genetics of the University Medical Center Groningen provided genomic DNA of 85 control subjects to exclude the possibility that detected second-site mutations were rare polymorphisms. All donors gave informed consent. Also, cDNA samples from dissected cells were subjected to nested PCR. All primers were designed in such way that the PCR product contained sequences from multiple exons (Supplemental Table 2). All PCR analyses were repeated with templates from at least 3 separate LDM-obtained nucleic-acid isolations. The resulting PCR products were cloned into the pCR4-TOPO vector (Invitrogen). For each revertant biopsy specimen, more than 10 clones were selected and sequenced.

Accession numbers. The GenBank accession numbers for the human *LAMB3* gene are U17744–U17760.

Acknowledgments

We are grateful to the patients and their families for their participation in this study. We thank José Duipmans and Miranda Nijenhuis for their excellent assistance. Part of this work was supported by the European GENESKIN coordinated action (LSHM-CT-2005-512117).

Received for publication September 26, 2006, and accepted in revised form February 6, 2007.

Address correspondence to: Marcel F. Jonkman, Center for Blistering Diseases, University Medical Center Groningen, Department of Dermatology, Hanzeplein 1, NL-9700 RB Groningen, The Netherlands. Phone: 31-50-361-2520; Fax: 31-50-361-2624; E-mail: m.f.jonkman@derm.umcg.nl.

1. Kvittingen, E.A., Rootwelt, H., Berger, R., and Brandtzaeg, P. 1994. Self-induced correction of the genetic-defect in tyrosinemia type-I. *J. Clin. Invest.* **94**:1657–1661.
2. Hirschhorn, R. 2003. In vivo reversion to normal of inherited mutations in humans. *J. Med. Genet.* **40**:721–728.
3. Jonkman, M.F., Nuijts, M.C., and van Essen, A.J. 2003. Natural repair mechanisms in correcting pathogenic mutations in inherited skin disorders. *Clin. Exp. Dermatol.* **28**:625–631.
4. Varki, R., Sadowski, S., Pfendner, E., and Uitto, J. 2006. Epidermolysis bullosa. I. Molecular genetics of the junctional and hemidesmosomal variants. *J. Med. Genet.* **43**:641–652.
5. Mavilio, F., et al. 2006. Correction of junctional epidermolysis bullosa by transplantation of genetically modified epidermal stem cells. *Nat. Med.* **12**:1397–1402.
6. Jonkman, M.F., et al. 1997. Revertant mosaicism in epidermolysis bullosa caused by mitotic gene conversion. *Cell.* **88**:543–551.
7. Darling, T.N., Yee, C., Bauer, J.W., Hintner, H., and Yancey, K.B. 1999. Revertant mosaicism: partial correction of a germ-line mutation in *COL17A1* by a frame-restoring mutation. *J. Clin. Invest.* **103**:1371–1377.
8. Schuilenga-Hut, P.H.L., et al. 2002. Partial revertant mosaicism of keratin 14 in a patient with recessive epidermolysis bullosa simplex. *J. Invest. Dermatol.* **118**:626–630.
9. Smith, F.J.D., Morley, S.M., and Mclean, W.H.I. 2004. Novel mechanism of revertant mosaicism in Dowling-Meara epidermolysis bullosa simplex. *J. Invest. Dermatol.* **122**:73–77.
10. Pasmooij, A.M.G., Pas, H.H., Deviaene, F.C.L., Nijenhuis, M., and Jonkman, M.F. 2005. Multiple correcting *COL17A1* mutations in patients with revertant mosaicism of epidermolysis bullosa. *Am. J. Hum. Genet.* **77**:727–740.
11. Cserhalmi-Friedman, P.B., et al. 1998. Restoration of open reading frame resulting from skipping of an exon with an internal deletion in the *COL7A1* gene. *Lab. Invest.* **78**:1483–1492.
12. Gache, Y., et al. 2001. Genetic bases of severe junctional epidermolysis bullosa presenting spontaneous amelioration with aging. *Hum. Mol. Genet.* **10**:2453–2461.
13. Pasmooij, A.M.G., et al. 2005. A very mild form of non-Herlitz junctional epidermolysis bullosa: BP180 rescue by outsplicing of mutated exon 30 coding for the COL15 domain. *Exp. Dermatol.* **13**:125–128.
14. Pulkkinen, L., et al. 1998. *LAMB3* mutations in generalized atrophic benign epidermolysis bullosa: consequences at the mRNA and protein levels. *Lab. Invest.* **78**:859–867.
15. Jonkman, M.F., et al. 1996. Generalized atrophic benign epidermolysis bullosa. Either 180-kd bullous pemphigoid antigen or laminin-5 deficiency. *Arch. Dermatol.* **132**:145–150.
16. Bliksrud, Y.T., Brodtkorb, E., Andresen, P.A., van den Berg, I.E.T., and Kvittingen, E.A. 2005. Tyrosinaemia type I — de novo mutation in liver tissue suppressing an inborn splicing defect. *J. Mol. Med.* **83**:406–410.
17. Wada, T., et al. 2005. Oligoclonal expansion of T lymphocytes with multiple second-site mutations leads to Omenn syndrome in a patient with RAG1-deficient severe combined immunodeficiency. *Blood.* **106**:2099–2101.
18. Marinkovich, M.P., Lunstrum, G.P., and Burgeson, R.E. 1992. The anchoring filament protein kalinin is synthesized and secreted as a high-molecular-weight precursor. *J. Biol. Chem.* **267**:17900–17906.
19. McGrath, J.A., et al. 1995. Altered laminin-5 expression due to mutations in the gene encoding the beta-3 chain (LAMB3) in generalized atrophic benign epidermolysis-bullosa. *J. Invest. Dermatol.* **104**:467–474.
20. Posteraro, P., et al. 1998. Compound heterozygosity for an out-of-frame deletion and a splice site mutation in the *LAMB3* gene causes nonlethal junctional epidermolysis bullosa. *Biochem. Biophys. Res. Commun.* **243**:758–764.
21. Wessagowit, V., Nalla, V.K., Rogan, P.K., and McGrath, J.A. 2005. Normal and abnormal mechanisms of gene splicing and relevance to inherited skin diseases. *J. Dermatol. Sci.* **40**:73–84.
22. Fairbrother, W.G., Yeh, R.F., Sharp, P.A., and Burge, C.B. 2002. Predictive identification of exonic splicing enhancers in human genes. *Science.* **297**:1007–1013.
23. Shen, L.X., Basilion, J.P., and Stanton, V.P., Jr. 1999. Single-nucleotide polymorphisms can cause different structural folds of mRNA. *Proc. Natl. Acad. Sci. U. S. A.* **96**:7871–7876.
24. Buratti, E., and Baralle, F.E. 2004. Influence of RNA secondary structure on the pre-mRNA splicing process. *Mol. Cell. Biol.* **24**:10505–10514.
25. Pulkkinen, L., et al. 1994. A homozygous nonsense mutation in the beta-3 chain gene of laminin-5 (LAMB3) in Herlitz junctional epidermolysis-bullosa. *Genomics.* **24**:357–360.
26. Dietz, H.C., et al. 1993. The skipping of constitutive exons *in vivo* induced by nonsense mutations. *Science.* **259**:680–683.
27. Rieux-Laucat, F., et al. 2006. Inherited and somatic CD3zeta mutations in a patient with T-cell deficiency. *N. Engl. J. Med.* **354**:1913–1921.
28. Hamanoue, S., et al. 2006. Myeloid lineage-selective growth of revertant cells in Fanconi anaemia. *Br. J. Haematol.* **132**:630–636.
29. Levran, O., et al. 1997. Sequence variation in the Fanconi anemia gene FAA. *Proc. Natl. Acad. Sci. U. S. A.* **94**:13051–13056.
30. Wikonkal, N.M., and Brash, D.E. 1999. Ultraviolet radiation induced signature mutations in photocarcinogenesis. *J. Investig. Dermatol. Symp. Proc.* **4**:6–10.
31. Nachman, M.W., and Crowell, S.L. 2000. Estimate of the mutation rate per nucleotide in humans. *Genetics*. **156**:297–304.
32. Levitt, N.C., and Hickinson, I.D. 2002. Caretaker tumour suppressor genes that defend genome integrity. *Trends Mol. Med.* **8**:179–186.
33. Frank, S.A., and Nowak, M.A. 2004. Problems of somatic mutation and cancer. *Bioessays.* **26**:291–299.
34. Pyke, C., et al. 1994. The gamma-2-chain of kalinin/laminin-5 is preferentially expressed in invading malignant-cells in human cancers. *Am. J. Pathol.* **145**:782–791.
35. Ryan, M.C., Tizard, R., Vandevanter, D.R., and Carter, W.G. 1994. Cloning of the Lama3 gene encoding the alpha-3-chain of the adhesive ligand epiligrin. Expression in wound repair. *J. Biol. Chem.* **269**:22779–22787.
36. O'Toole, E.A., Marinkovich, M.P., Hoeffler, W.K., Furthmayr, H., and Woodley, D.T. 1997. Laminin-5 inhibits human keratinocyte migration. *Exp. Cell Res.* **233**:330–339.
37. Decline, F., and Rousselle, P. 2001. Keratinocyte migration requires alpha 2 beta 1 integrin-mediated interaction with the laminin 5 gamma 2 chain. *J. Cell Sci.* **114**:811–823.
38. Yuen, H.W., et al. 2005. Suppression of laminin-5 expression leads to increased motility, tumorigenicity, and invasion. *Exp. Cell Res.* **309**:198–210.
39. Jonkman, M.F., et al. 1995. 180-kD bullous pemphigoid antigen (BP180) is deficient in generalized atrophic benign epidermolysis-bullosa. *J. Clin. Invest.* **95**:1345–1352.